

# Electric and magnetic response of Li-doped $\text{YBa}_2\text{Cu}_3\text{O}_{7-x}(\text{LiF})_x$ under neutron irradiation

V. SANDU<sup>\*</sup>, G. ALDICA, E. SANDU<sup>a</sup>, P. NITA<sup>b</sup>

*National Institute of Materials Physics, 105 b Atomistilor, Magurele, 077125 Romania*

*<sup>a</sup>National Institute of Physics and Nuclear Engineering "Horia Hulubei", 407 Atomistilor, Magurele, 077125 Romania*

*<sup>b</sup>METAV SA, 67-77 Biharia, Bucharest, 013981, Romania*

We investigate the effect of neutron irradiation on the electric and magnetic properties, including the enhancement of the critical current density, of ceramics  $\text{YBa}_2\text{Cu}_3\text{O}_{7-x}(\text{LiF})_x$  samples. The most important finding has been that the level of Li-doping is crucial for the postirradiation response. The irreversibility increases for more than two times in the samples with  $x \leq 0.04$  after neutron irradiation at  $5 \times 10^{17}$  neutrons/cm<sup>2</sup> but less for higher concentrations. The effects of the irradiation on the electric transport and *ac*-susceptibility suggest a self-organization of the defects at low Li content and a uniformly space distribution for  $x \geq 0.08$ .

(Received January 9, 2007; accepted December 4, 2007)

*Keywords:*  $\text{YBa}_2\text{Cu}_3\text{O}_7$ , neutron irradiation, Self-organization, Critical current density, Magnetization

## 1. Introduction

High temperature superconductors (HTS) have a weak pinning generated by the point disorder related mainly to the oxygen vacancies. Therefore, vortex lines meanders among the pinning points in order to minimize the total free energy which consists of three competing terms: the pinning energy, line energy, and vortex-vortex interactions. Extended defects that grab hold of vortex lines along the length of the defect, hence, display extensive character, provide an enhanced pinning energy as long as the elastic cost due to the line energy is moderate. The pinning energy of a single vortex line has a square root growth with the length of the pinning energy when the flux line meanders among pinning points [1] and increases linearly when it is properly aligned with an extended defect [2].

Natural examples of extended defects in high temperature superconductors are twin boundaries point defect loops or any other type of dislocation expected in crystals. They attract vortices, limit their motion to a specific direction or lock them in. Additionally, the reduced dimensionality of the motion reduces in turn the thermal fluctuations. Therefore, this kind of defects is most wanted in the systems dedicated to large scale applications. Usually, their density is not very high; hence, the effect on pinning is marginal. For that reason, the generation of extended defects in an artificial way is preferred.

The main method used to create extended defects is particle irradiation. During irradiation, the accumulation of defects is strongly dependent on the underlying sample morphology and grain structure. Specifically, irradiation can trigger the defect accumulation in a uniform way for a density of dislocation and/or vacancy loops higher than a critical value or can generate patterns in the opposite case [3]. Generally, a uniform distribution of the extended defects has suppressive effects on superconductivity, while

the latter generates a local improvement of the superconducting properties.

Neutrons are very appropriate to generate bulk defects owing to their electric neutrality. When thermal neutrons are the main component of the neutron beam, the capture process dominates the interactions with the atomic species that make up the target structure. Unfortunately, in the case of the most used HTS, the constitutive atoms have an effective cross section to neutron capture  $\sigma$  of order unity. Consequently, atoms with high  $\sigma$  have to partially substitute for some atoms of HTS in manner that leaves the superconductivity unaltered. Previous investigations showed that lithium is very appropriate for this job because its isotope <sup>6</sup>Li has an effective cross section  $\sigma = 936$  barn, a natural abundance of 17% and is not poisonous for superconductivity [4]. The most efficient compound to transfer Li in HTS is the use of Li-halides as vector [5]. The amount of Li compound inserted during the fabrication is also important for the morphostructure of the ceramic sample. Therefore, one can use the level of Li to impose a particular evolution of defect accumulation within grains. In this paper, we present the effects of neutron irradiation on Li-doped  $\text{YBa}_2\text{Cu}_3\text{O}_{7-x}$  ceramic samples in which Li was inserted via lithium fluoride. Using different concentration of Li, we found out responses which reflect either the uniform accumulation of defects or the domain formation.

## 2. Experimental

$\text{YBa}_2\text{Cu}_3\text{O}_{7-x}(\text{LiF})_x$  ceramic samples,  $x = 0.02; 0.04;$  and  $0.08$ , were prepared by solid state reaction from high grade reagents as presented elsewhere [5]. The halide was mixed with stoichiometric  $\text{YBa}_2\text{Cu}_3\text{O}_{7-x}$  powder and sintered in flowing oxygen at temperatures lower with 10 to 20 °C than the sintering temperature of the pure cuprate. The irradiation of the samples was performed at the INR

Pitesti 14MW TRIGA reactor at a fluence of  $5 \times 10^{17}$  neutrons/cm<sup>2</sup>. The samples were sealed in quartz ampoules and suspended in the reactor core. After irradiation the samples were stored for one month to reduce the residual activity at the level accepted for public (1 mSv/year). The samples were further submitted to complex investigations regarding the magnetic and transport properties. Transport investigation was made using the four point method whereas magnetization was measured only at 77 K. The *ac*-susceptibility was measured with a home made susceptometer. The morphology of the samples was investigated with a Hitachi S-2600N scanning electron microscope before and after irradiation.

### 3. Results and discussions

Fig. 1 shows the temperature  $T$  dependence of the resistivity  $\rho$  for the virgin samples. There are several peculiarities that will be mirrored in the response to neutron irradiation. At room temperature, the addition of lithium decreases the resistivity at high temperature. A reason should be the enhancement of the sintering process at high temperature because LiF provides wet channels increasing the diffusion process, and, subsequently, better intergrain contacts.

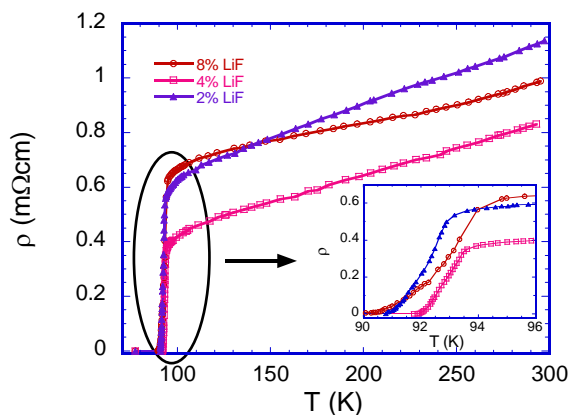
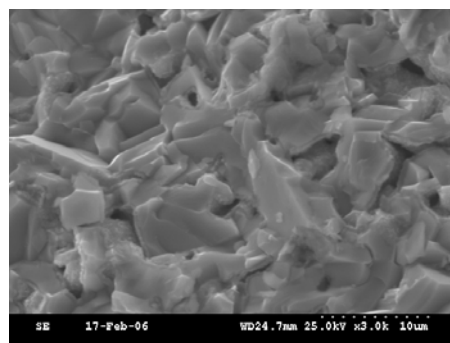


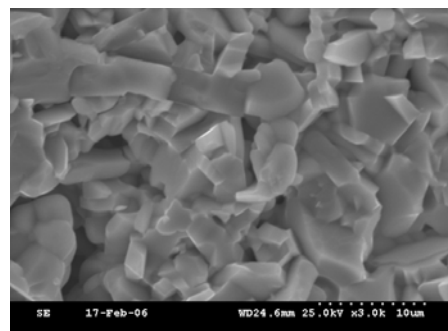
Fig. 1. Temperature dependence of the resistivity of the virgin samples of  $\text{YBa}_2\text{Cu}_3\text{O}_{7-\delta}$  doped with Li via LiF. Inset: The superconducting transition.

However, too much Li compound could substitute Li for Cu and reduces the hole-doping. Therefore there is an optimal doping that we find to occur at  $x \approx 0.04$ . For this level of Li-doping we obtained the highest temperature and the lowest residual resistance. The samples with  $x = 0.02$  and  $0.04$  depend linearly on  $T$  which is typical for the optimally doped cuprates. The derivative clearly shows a two-stepped transition (data not shown) mirroring, most likely, the grain and intergrain transitions, respectively. This biphasic structure was further confirmed by *ac*-susceptibility data (see Figs. 7 below). The sample with 8% LiF has a two times wider superconducting transition. Moreover, the transition shows a decrease of  $d\rho/dT$  just before the superconducting transition which is distinctive

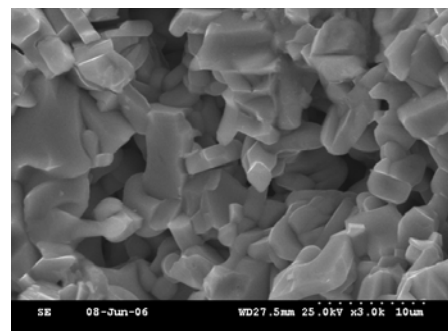
for underdoped HTS. These assumptions are supported by SEM micrographies. In the case of  $x = 0.02$  (Fig. 2 a), the structure is almost homogeneous, with uniformly sized polyhedral grains and a high density of pores of average size of  $1 \mu\text{m}$  with both inter and intragranular location. For  $x = 0.04$  (Fig. 2 b). Voids of size  $10 - 30 \mu\text{m}$  appear more frequently. The grain structure is less homogeneous but they display adherences of the grain borders that confer a higher degree of local compactness. At the highest LiF content ( $x = 0.08$ ) the structure is nonuniform (Fig. 2 c) with a high density of voids and molten areas. The conclusion is that an increased LiF addition produces clusters of well connected grains, but the cost is an increased inhomogeneity. As long as the connectivity effects prevail, the transport properties are enhanced, even though it seems that they are more or less of percolative type.



a



b



c

Fig. 2. SEM micrographs of  $\text{YBa}_2\text{Cu}_3\text{O}_{7-\delta}(\text{LiF})_x$  ( $\times 3000$ ). a)  $x = 0.02$ ; b)  $x = 0.04$ ; and c)  $x = 0.08$ .

After irradiation, the transport properties display different evolutions though the resistivity increases for all samples. The samples with a higher structural homogeneity show a 0.9 K increase of the postirradiation critical temperature (Figs. 3) accompanied by a slight decrease of the transition width. The residual resistivity doubles up, as well as the slope  $d\rho/dT$ . However, a quadratic contribution is present at  $x = 0.04$  as in overdoped samples (Inset to Fig. 3b).

The salient improvement of the superconducting transition after irradiation is not in contradiction with the general increase of the resistivity in normal state. Indeed, in a ceramic sample, both the grains and the grain border contribute to the total resistivity. Usually, the resistivity of the grain is lower than the grain border. Therefore, the grain border acts like a valve controlling the charge transport. The two contributions might behave differently under neutron irradiation; the most influenced being the border area. A study on Li inserted via LiCl,[6] which has similar effects as LiF, have revealed a slight increase of the grains and grain uniformity after irradiation.

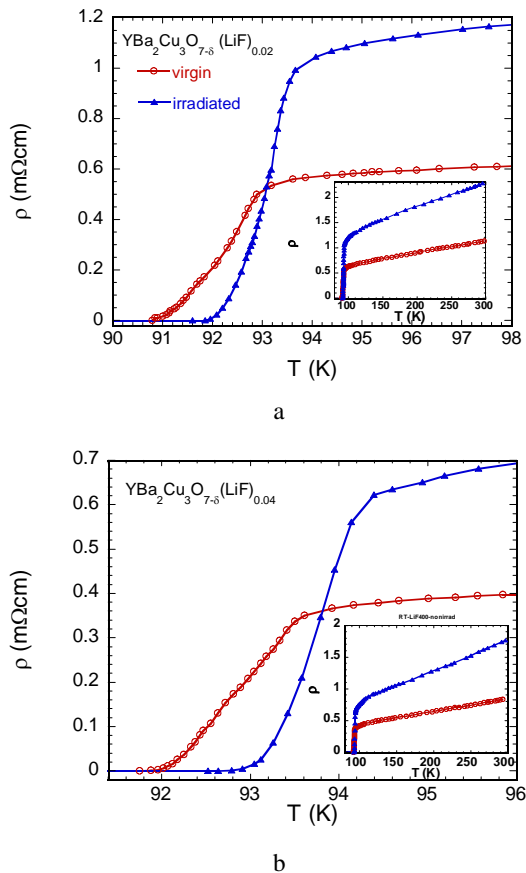


Fig. 3. Temperature dependence of the resistivity of  $YBa_2Cu_3O_{7-\delta}(LiF)_x$  before and after neutron irradiation at  $5 \times 10^{17}$  neutrons/cm<sup>2</sup>. a) sample with  $x = 0.02$ ; b) sample with  $x = 0.04$ . Insets: the same plot on an extended  $T$  range.

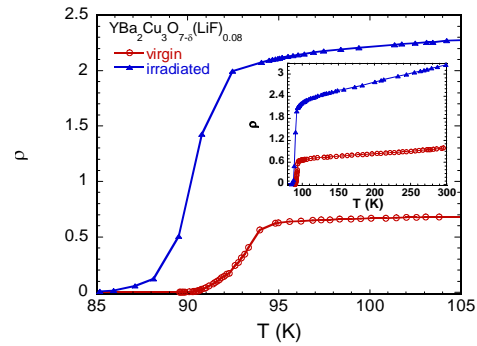


Fig. 4. Temperature dependence of the resistivity of  $YBa_2Cu_3O_{7-\delta}(LiF)_{0.08}$  before and after neutron irradiation at  $5 \times 10^{17}$  neutrons/cm<sup>2</sup>. Inset: the same plot on an extended  $T$  range.

The sample with  $x = 0.08$  has a different dependence on irradiation. The normal state resistivity is multiplied by two after irradiation whereas the critical temperature is depressed with 2.8 K (Fig. 4). It is interesting that the sample recovers the linearity of  $\rho$  vs  $T$  dependence after irradiation (see Inset to Fig. 4). The degradation of the critical temperature suggests that the mechanisms of superconductivity itself are influenced within grain by the energy deposited in the sample subsequent the interaction with the neutrons.

Isothermal magnetization data at 77 K (Fig. 5) show a reduction of the asymmetry of the hysteresis loops both with increasing the Li content and neutron fluence.

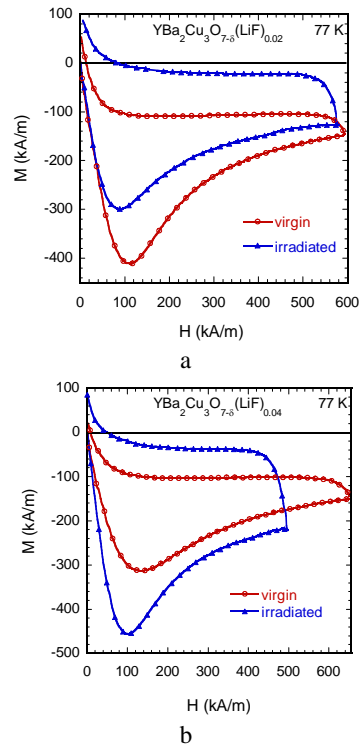


Fig. 5. Magnetization hysteresis loops at 77 K of  $YBa_2Cu_3O_{7-\delta}(LiF)_x$  samples before and after neutron irradiation at  $5 \times 10^{17}$  neutrons/cm<sup>2</sup>. a) sample with  $x = 0.02$  sample with  $x = 0.04$ .

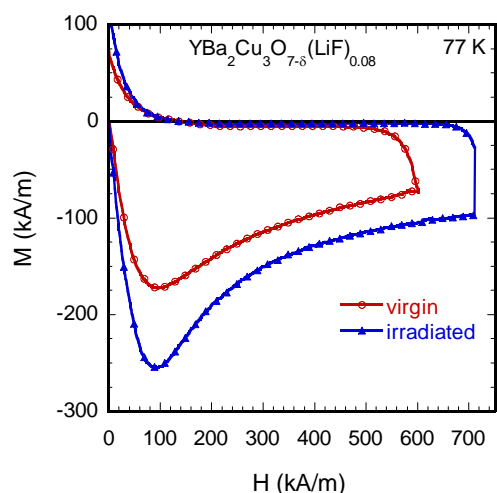


Fig. 6. Isothermal magnetization loops at 77 K of ceramic  $\text{YBa}_2\text{Cu}_3\text{O}_{7-x}(\text{LiF})_{0.08}$  before and after neutron irradiation at  $5 \times 10^{17}$  neutrons/cm<sup>2</sup>.

The asymmetry in the case of the virgin samples is connected to the Bean-Livingstone barriers [7-9] which appear at good surfaces. The addition of Li might suppress the superconducting order parameter at the grain surface creating weak points for the penetration of flux lines, hence, it destroys the barriers, which is most striking for the sample containing  $x = 0.08$ .

The irradiation is more effective in destroying the effect of surface [10]. Actually, it is just the effect of the uniform dissemination of pinning centers within sample, including the grains and their border area. Obviously, the most spectacular effect is the increase of the irreversibility, hence, of the intragranular critical current density. For the sample with low Li-content,  $x \leq 0.04$  the critical current density doubles up.

For more lithium, the increase of the irreversibility is conspicuous but less spectacular than for lower Li content (Fig. 6). However, the irradiation does not show a significant enhancement of the surface pinning.

AC-susceptibility data  $\chi$  confirm the results of the transport and magnetization measurements. Figs. 7 show the imaginary part of ac-susceptibility  $\chi''$  that reflects the increase of the irreversibility as well as the evolution of the superconducting phases under neutron irradiation.

In the case of the samples with low Li content, the biphasic structure of the as prepared samples, which is also visible in the  $\rho$  vs  $T$  plots, changes to a single phase system and shifts to higher temperatures (Fig. 7a and 7b). Additionally, the irreversibility increases in a spectacular way.

The behavior of the sample with  $x = 0.08$  is different under the energy deposited by neutrons. The irreversibility increases, the biphasic structure changes in a single one, like in the case of the samples with lower amount of Li,

but the peak temperature shifts to lower temperature in agreement with  $T$  dependence of the resistivity (Fig. 7c).

The doping dependent response to neutron irradiation is the result of the complex formation, evolution, and stability of defects microstructures. The defects created by irradiation move by diffusion or gliding, recombine, are captured, or released with a rate dependent of the defect dimension. The result is a strongly nonlinear process able to give rise to self-organization of the defects, a process in which the initial underlying structure of the sample is crucial. Walgraef and Ghoniem [3] have shown that, for a low density of network dislocations, the uniform distribution of defects may become unstable relative to the pattern formation. Actually, this is the effect of the difference of the mobility of the Frankel defects and of the bias of the line defects (vacancy loops and dislocation networks). The pattern formation is enhanced in the anisotropic systems most likely in the basal planes where the mobility of the interstitial is larger. The patterns would consist in walls made of clusters of dislocations separating dislocation free areas. When the wavelength of the pattern is of the order of the grain size, the grain remain almost defect free expelling the walls in the vicinity of the grain border. The increase of the fluence keeps accumulating the defects within the walls (*higher harmonics effect* [11]). The effect is important in the samples with a low Li content. They have a low density of surface defects as the asymmetry of the hysteresis loops shows (Figs. 5a and 5b), and, accordingly, a low density of intragrain defects. Therefore, it is expected that defect self-organization occurs within grains. The shape and size of the grains impose the position of the walls where the defects build up, most likely at the grain border. The formation of walls explains the increase of the normal state resistivity as well as of the residual resistivity observed in all samples (see Figs. 3). The increase of the critical temperature and the transformation of the imaginary part of the ac-susceptibility from a double peaked and large curve to a narrow and well peaked one (Fig. 7a and 7b) mirror the evolution to an intragranular structure with defect-free areas of size not larger than the crystal grains triggered by neutron irradiation.

The circumstances are different for  $x = 0.08$ , a sample with many voids (Fig. 2c) and melt zones, and grain surface less perfect than in previous cases (Fig. 6) in virgin state. The decrease of the critical temperature after irradiation (Fig. 3c) shows that there is no self-organization in this sample, but the energy deposited by irradiation might produce an annealing which produces a homogenization of the phase structure (Fig. 4 and Fig. 7c). The decrease of the critical temperature, shows, however, that the fundamental mechanisms of superconductivity are disturbed. The effect is weak but obvious.

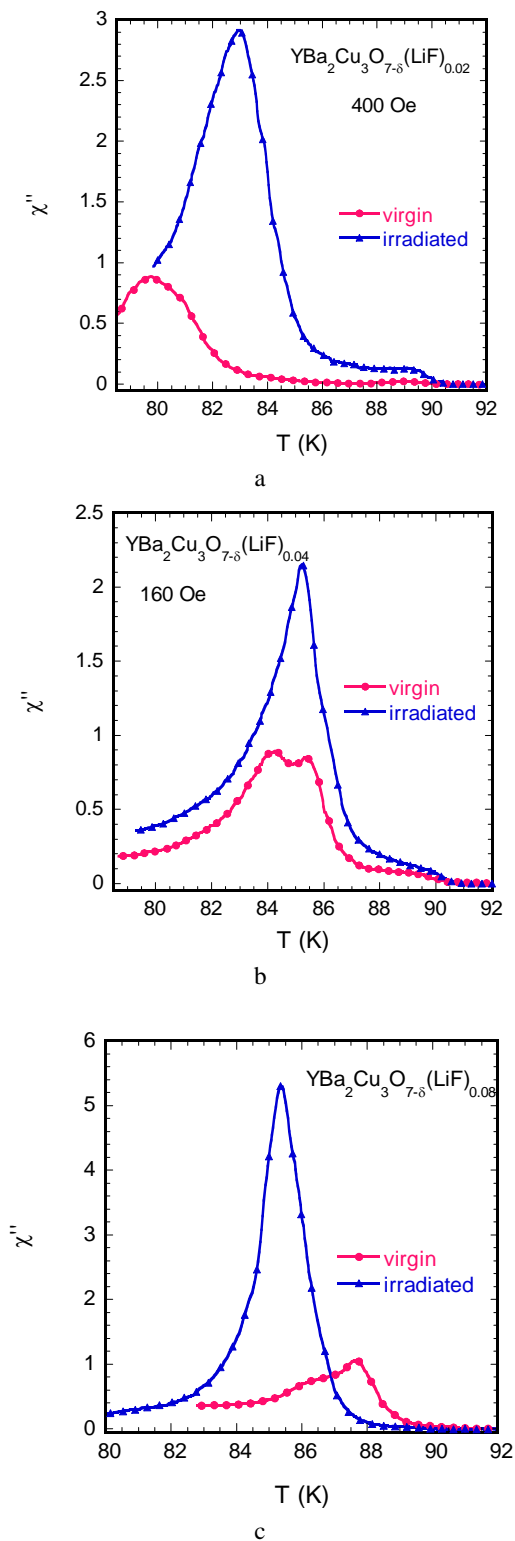


Fig. 7. Temperature dependence of the imaginary part of ac-susceptibility of ceramic  $\text{YBa}_2\text{Cu}_3\text{O}_{7-\delta}(\text{LiF})_x$  samples before and after neutron irradiation at  $5 \times 10^{17}$  neutrons/cm<sup>2</sup>. a)  $x = 0.02$  at an applied field of 400 Oe; b)  $x = 0.04$  at an applied field of 160 Oe; c)  $x = 0.08$  at zero field.

It is not clear which kind of defect is responsible for the spectacular increase of the critical current density in all samples. Twin or dislocation loops, as extended defects, enhanced by the increase of the superconductivity in the rest of the grain are the most plausible candidates.

To summarize, we have investigated the evolution of Li-doped  $\text{YBa}_2\text{Cu}_3\text{O}_7$  under neutron irradiation. We established a doping dependence of the electric and magnetic response which reflects different evolution of the defect structure subsequent irradiation. The samples with low lithium content ( $x \leq 0.04$ ) display a response which suggests a process of self-organization of the defects in thin walls edging larger defect-free areas whereas the sample with high amount of Li show a decrease of the superconducting properties in agreement with an uniform distribution of the irradiation generated defects.

### Acknowledgments

The research was supported by the Romanian NARS under the Projects CEEX 73 at NIMP.

### References

- [1] I. Larkin, Yu. N. Ovchinnikov, Zh. Eksp. Teor. Fiz. **65**, 1709 (1973); J. Low Temp. Phys. **34**, 409 (1979).
- [2] G. Blatter, J. Rhyner, V. M. Vinokur, Phys. Rev. **B 43**, 7826 (1991).
- [3] D. Walgraef, N. M. Ghoniem, Phys. Rev. **B 39**, 8867 (1989).
- [4] V. Sandu, J. Jaklovszky, Gh. Aldica, E. Cimpoiasu, M. C. Bunesu, Balkan. Phys. Lett. **6**, 238 (1998).
- [5] V. Sandu, J. Jaklovszky, E. Cimpoiasu, M. C. Bunesu, J. Supercond. **11**, 653 (1998).
- [6] Unpublished data provided by P. Nita.
- [7] C. P. Bean, J. D. Livingston, Phys. Rev. **B 12**, 14 (1964).
- [8] L. Burlachkov, M. Konczykowski, Y. Yeshurun, F. Holtzberg, J. Appl. Phys. **70**, 5759 (1991).
- [9] N. Chikumoto, M. Konczykowski, N. Motohira, A. P. Malozemoff, Phys. Rev. Lett. **69**, 1260 (1992).
- [10] M. Konczykowski, L. Burlachkov, Y. Yeshurun, F. Holtzberg, Phys. Rev. **B 43**, 13707 (1991).
- [11] D. Walgraef, J. Lauzeral, N. M. Ghoniem, Phys. Rev. **B 53**, 14782 (1996).

\*Corresponding author: vsandu@infim.ro